DISCOVERY OF A SUBPARSEC RADIO COUNTERJET IN THE NUCLEUS OF CENTAURUS A

DAYTON L. JONES,[1] STEVEN J. TINGAY,[2] DAVID W. MURPHY,[1] DAVID L. MEIER,[1] DAVID L. JAUNCEY,[3] JOHN E. REYNOLDS,[3]
ANASTASIOS K. TZIOUMIS,[3] ROBERT A. PRESTON,[1] PETER M. MCCULLOCH,[4] MARCO E. COSTA,[4] ATHOL J. KEMBALL,[5]
GEORGE D. NICOLSON,[5] JONATHAN F. H. QUICK,[5] EDWARD A. KING,[4] JAMES E. J. LOVELL,[4] R. W. CLAY,[6]
RICHARD H. FERRIS,[3] R. G. GOUGH,[3] M. W. SINCLAIR,[3] S. P. ELLINGSEN,[4] P. G. EDWARDS,[7]
P. A. JONES,[8] T. D. VAN OMMEN,[9] PAUL HARBISON,[10] AND VICTOR MIGENES[11]
Received 1996 April 25; accepted 1996 May 23

ABSTRACT

A subparsec scale radio counterjet has been detected in the nucleus of the closest radio galaxy, Centaurus A (NGC 5128), with VLBI imaging at 2.3 and 8.4 GHz. This is one of the first detections of a VLBI counterjet and provides new constraints on the kinematics of the radio jets emerging from the nucleus of Cen A. A bright, compact core is seen at 8.4 GHz, along with a jet extending along P.A. 51°. The core is completely absorbed at 2.3 GHz. Our images show a much wider gap between the base of the main jet and the counterjet at 2.3 GHz than at 8.4 GHz and also that the core has an extraordinarily inverted spectrum. These observations provide evidence that the innermost 0.4–0.8 pc of the source is seen through a disk or torus of ionized gas which is opaque at low frequencies due to free-free absorption.

Subject headings: accretion, accretion disks — galaxies: active — galaxies: individual (NGC 5128, Centaurus A) — galaxies: jets — galaxies: nuclei

1. INTRODUCTION

Observations of radio galaxies generally reveal a strong asymmetry in surface brightness close to the central radio source (associated with the nucleus of the host galaxy) and more symmetric structure at larger distances. An attractive explanation for these observations is that the inner structure is intrinsically symmetric—two oppositely directed, relativistic jets of radio emitting plasma—but appears asymmetric due to relativistic beaming (amplification) of the emission in the direction of jet motion. If the jet material is decelerated between the nucleus and the large-scale radio lobes, the effect of beaming is reduced, and the true symmetry of the source becomes apparent far from the nucleus.

A simple expression describes the ratio of observed surface brightness from approaching and receding radio components (R) in terms of the bulk velocity of material in the jet ($\beta \equiv v/c$) and the angle between the approaching jet axis and our line of sight (θ):

$$R = \left[\frac{1 + \beta \cos \theta}{1 - \beta \cos \theta} \right]^{3-\alpha}$$

[1] Jet Propulsion Laboratory, Mail Code 238-332, California Institute of Technology, 4800 Oak Grove Drive, Pasadena, CA 91109; dj@bllac.jpl.nasa.gov.
[2] Mount Stromlo and Siding Spring Observatories, Australian National University, Private Bag, Weston Creek Post Office, ACT 2611, Australia; tingay@merlin.anu.edu.au.
[3] Australia Telescope National Facility, CSIRO, P.O. Box 76, Epping, NSW 2121, Australia.
[4] University of Tasmania, G.P.O. 252C, Hobart, Tasmania 7001, Australia.
[5] Hartebeesthoek Radio Astronomy Observatory, P.O. Box 443, Krugersdorp 1740, Transvaal, South Africa.
[6] University of Adelaide, Adelaide, SA, Australia.
[7] Institute of Space and Astronautical Science, 3-1-1, Yoshinodai, Sagamihara-shi, Kanagawa 229, Japan.
[8] University of Western Sydney, Kingswood, NSW, Australia.
[9] Antarctic Cooperative Research Centre, University of Tasmania, Hobart, TAS, Australia.
[10] British Aerospace Australia, Canberra, ACT, Australia.
[11] National Astronomical Observatory, Mitaka-shi, Tokyo 181, Japan.

for isotropic emission in the rest frame of the jet (Ryle & Longair 1967). Here α is the radio spectral index of the jet defined as $S_\nu \propto \nu^\alpha$ where S_ν is the flux density at frequency ν. (An exponent of $2 - \alpha$ is appropriate if the jet is modeled as a continuous flow of material instead of a series of separate knots of radio-emitting plasma [Scheuer & Readhead 1979].) Detection of a counterjet places constraints on β and θ and is important in testing unification schemes based on beaming and orientation arguments.

NGC 5128 is the closest "classical" radio galaxy, only 3.5 Mpc distant (Hui et al. 1993). The proximity of this active galaxy allows higher linear resolution imaging than can be obtained for more distant galaxies. It is not an intrinsically high luminosity radio source, but can be studied over a very wide range of linear scales due to its proximity. The extended radio emission associated with Cen A covers an area of $8°.5 \times 3°.5$ on the sky (Junkes et al. 1993), while observations with VLBI arrays can obtain images of the nuclear radio source in this galaxy with angular resolution of 1 mas or better (corresponding to a linear resolution of less than 0.02 pc). The large-scale radio morphology of Cen A, along with its low intrinsic radio power, suggests a moderate-speed jet oriented close to the plane of the sky. Therefore, this source is a good candidate for detection of a VLBI counterjet.

2. OBSERVATIONS AND RESULTS

At decl. −43°, Cen A is well placed for observations with Southern Hemisphere VLBI Experiment (SHEVE) antennas in Australia and South Africa combined with several antennas of the Very Long Baseline Array (VLBA). This combination provides better coverage of the aperture plane than either SHEVE or the VLBA alone. Our 8.4 GHz observations were made on 1993 October 20 using the SHEVE array and five VLBA antennas in the southwestern US. The resulting image is shown in Figure 1.

Three things are immediately noticeable in the 8.4 GHz image: the jet is nearly linear and oriented along the position
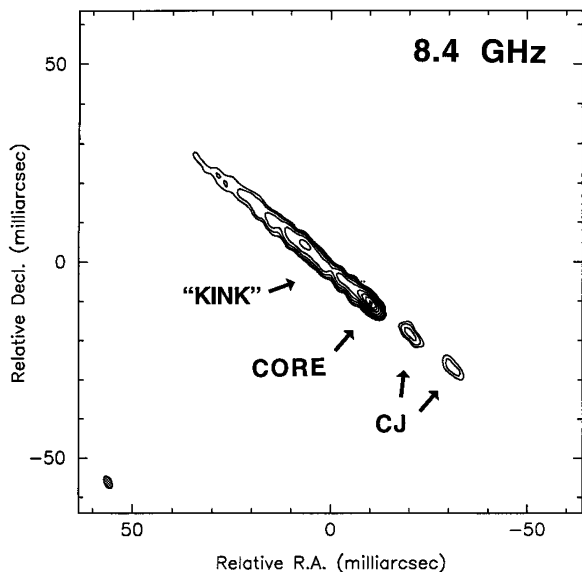
FIG. 1.—8.4 GHz VLBI image of the nucleus of Cen A in 1993 October, made with antennas in Australia, South Africa, and the United States. North is up; east is to the left. The brightest peak corresponds to the inverted-spectrum core, and the counterjet peaks are located to the southwest of the brightest peak. Note also the slight wiggle or kink in the main jet 15–20 mas northeast of the brightest peak. The contour levels are −1, 1, 2, 4, 8, 16, 32, 50, 70, and 95% of the peak brightness (1.80 Jy beam^{-1}). The restoring beam (*lower left corner*) is 3.22×1.82 mas with the major axis in P.A. $26°2$.

FIG. 2.—2.3 GHz SHEVE image of the nucleus of Cen A in 1988 November, made with six antennas in Australia. The contour levels are −1, 1, 2, 4, 8, 16, 32, 50, 70, and 95% of the peak brightness (1.43 Jy beam^{-1}). The orientation and scale of this figure are the same as in Figure 1. The restoring beam is 7.26×5.53 mas with the major axis in position angle $8°5$. The brightest peak in this image corresponds to the "kink" in Figure 1, and the approximate location of the (absorbed) core is marked.

angle of the larger scale jet seen in VLA images (51°), the peak brightness occurs at the "base" (southwest end) of the continuous jet, and there are two isolated peaks of emission approximately 12 and 27 mas southwest of the brightest peak. We associate these peaks with an underlying counterjet because of their location along the same position angle as the main jet on the opposite side of the core (determined from a comparison of 4.8 and 8.4 GHz VLBI images, as described below). We also note the presence (in VLA images) of other isolated knots of emission farther from the core and in the direction of the southwest inner radio lobe (Clarke, Burns, & Norman 1992).

How do we know that one of the features we associate with a counterjet is not really the core? Absolute registration of VLBI images at different frequencies is not generally possible, but a comparison of nearly simultaneous images (separated by 3 days during 1992 November) at 4.8 and 8.4 GHz shows a distinctive "kink" in the main jet 16 mas northeast of the brightest peak at 8.4 GHz (see Fig. 1 in Jauncey et al. 1995). Aligning this feature on both images shows that the bright peak at the base of the main jet at 8.4 GHz has a highly inverted spectrum, while the rest of the main jet has a spectrum ranging from less inverted to flat to steep with increasing distance from the core (Jauncey et al. 1995). Other alignments produce nonphysical spectral indices. It is possible that the counterjet also has an inverted spectrum (due, for example, to free-free absorption in a nuclear disk of gas), but a higher quality 4.8 GHz image will be needed to test this hypothesis. The present 4.8 GHz data have a limited dynamic range and are only sufficient to constrain the brightest regions of the source. However, single-antenna flux density measurements show that the brightness of the nucleus increases rapidly with frequency up to ≈ 22 GHz, indicating that the core does have an inverted spectrum at lower frequencies (Beall et al. 1978). Since the inverted-spectrum core still dominates the
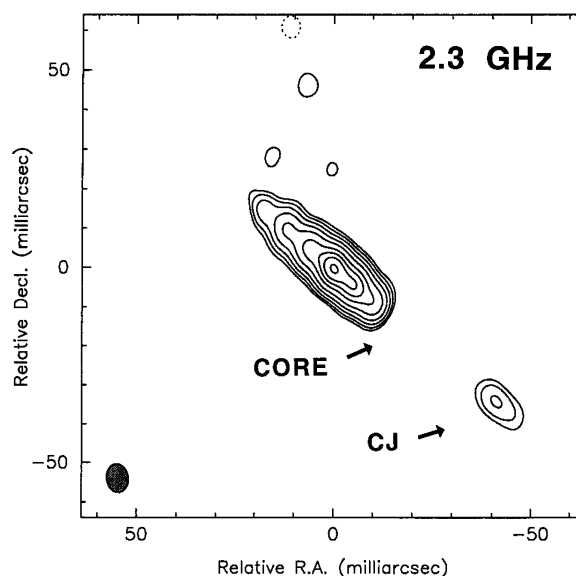
total nuclear flux density at 8.4 GHz, the brightest peak on our 8.4 GHz image, which is also the only unresolved feature in the image, is indeed the core.

Figure 2 shows a SHEVE image from observations made at 2.3 GHz on 1988 November 10. Single-antenna flux density measurements indicate that the true core is completely absorbed at this frequency. The bright jetlike feature in Figure 2 can be identified with the main jet seen at 8.4 GHz, with the brightest peak at 2.3 GHz identified with the "kink" in the jet at 8.4 GHz. The registration implied by this identification is the only physically reasonable one; shifting the 2.3 GHz image by a single beamwidth produces spectral indices which are implausibly steep or inverted. Additional evidence for the registration suggested here comes from simultaneous 2.3 and 8.4 GHz VLBA observations made in 1995 July. These observations are not of sufficient quality to show the counterjet clearly, but the same over-all structure as in Figures 1 and 2 is evident. Therefore morphological changes between the epochs of Figures 1 and 2 are not likely to have affected the large-scale spectral index distribution.

3. DISCUSSION

It is well known that self-calibration of VLBI data can produce symmetric structure about bright features even if the true source brightness distribution is asymmetric (Linfield 1986). This can occur when phases are self-calibrated with a point-source model, and either the quantity of data or the number of self-calibration iterations is insufficient to correct the initial symmetric bias introduced into the source model. As a result, most features which appear to be short counterjets in VLBI images are dismissed as being caused by residual errors in the self-calibrated data. The counterjet seen in Figures 1 and 2 differs from most calibration artifacts in that it is not an extension of (or immediately next to) a bright feature.

To test the reality of the counterjet, we reimaged the source without allowing any CLEAN components on the counterjet side during any of the self-calibration and deconvolution steps. After the strong main jet features were included in the model the brightest residuals were always in the positions of the counterjet features during every iteration at both 2.3 and 8.4 GHz. Allowing CLEAN components in this region increased the peak brightness of these features by a factor of 2, and improved the over-all fit of the model to the visibilities by more than 10% compared to the best one-sided source models. The counterjet peaks are seen separately in Mark-II and Mark-III data recorded during the 8.4 GHz experiment. We have also carried out blind imaging tests using simulated data to verify that our VLBI array provides sufficient coverage of the aperture plane to allow reliable imaging of features similar to those seen in Figure 1. In no case during these blind tests were counterjets created where none existed in the starting models. Finally, our data were imaged independently by three of the authors, resulting in virtually identical images.

There is some uncertainty in the registration of the images in Figures 1 and 2, but any realistic registration shows that the separation between the core and the first detectable feature in the counterjet is far greater at 2.3 GHz than at 8.4 GHz. This is not caused by changes in source morphology during the interval between our 2.3 and 8.4 GHz observations unless proper motions within the counterjet are far greater than those measured for bright features in the main jet. In addition, the spectrum of the core is highly inverted ($\alpha \sim 4$) between these two frequencies. An analysis of 4.8 and 8.4 GHz images by Tingay (1996) also finds a spectral index ≈ 4 for the core. Both of these effects can be explained if the central $0.4-0.8$ pc of Cen A is seen through a disk or torus of thermal gas inclined at a large angle to our line of sight. A similar situation has been found in 3C84 (Vermeulen, Readhead, & Backer 1994; Walker, Romney, & Benson 1994). For example, a 1–2 pc path through 10^4 K gas with electron density of 10^5 cm^{-3} will give a spectral turnover frequency greater than 15 GHz due to free-free absorption. The observed spectral index of about 4 at frequencies below 8.4 GHz would then correspond to an intrinsic spectral index of $2.0-2.5$ for the core, consistent with synchrotron self-absorption. If this model is correct, the inner part of the counterjet will be reduced in brightness by a factor of 13 more at 2.3 GHz than at 8.4 GHz, which would explain why we do not detect any 2.3 GHz emission at the locations of the 8.4 GHz counterjet features.

The jet/counterjet brightness ratio R is difficult to determine from only the brightest peaks of the counterjet. Comparison of the peak counterjet brightness to the main jet brightness at the same distance from the core gives $R \simeq 4$ at 8.4 GHz. However, if we use the brightest peak along the main jet for our comparison, values of R up to ~ 8 are obtained. The most appropriate comparison is between the brightness of the underlying (smooth?) jet and counterjet emission, not between the brightness of specific knots, but this must await the

availability of higher dynamic range VLBI images. Directly measured proper motions in the main jet are slow ($\approx 0.15c$; Jauncey et al. 1995; Tingay et al. 1994), but rapid changes in the size and brightness of individual jet components suggests that the flow speed of the jet is significantly faster ($\beta_{app} \geq 0.85$; Preston et al. 1996). The slower speed is inconsistent with the observed jet/counterjet bright ratio ($R \leq 8$), but the faster speed implied by component variability is consistent with the brightness ratio for a range of angles to our line of sight ($60°-77°$). Such an orientation is consistent with the large-scale radio morphology of Cen A. This model implies that the bulk flow speed of the jet need be only moderately relativistic ($\geq 0.66c$).

4. CONCLUSIONS

VLBI observations of many sources have been made to search for parsec-scale counterjets, which are predicted by the standard twin-beam model of radio sources in active galactic nuclei. However, the vast majority of radio sources observed with VLBI are high luminosity (FR II; Fanaroff & Riley 1974) objects, in which the jets are expected to be highly relativistic and oriented closer to our line of sight (in flux limited samples). Consequently, the effects of beaming lead to very large values of R and (currently) undetectable counterjets. Cen A, in contrast, is a lower luminosity FR I radio source. If there is a correlation between jet speed and total source luminosity, as suspected (Bridle & Perley 1984), then FR I sources should have much smaller values of R than FR II sources at the same angle to our line of sight. In the case of Cen A we also benefit from having a relatively large angle between the radio axis (as estimated from the large-scale morphology of the source) and our line of sight. Thus, the discovery of a parsec-scale radio counterjet in this source (and not in many other well-observed sources) is readily explained.

We are continuing to observe the nucleus of Cen A with SHEVE and the VLBA. With multiple epochs, it should be possible to measure the apparent proper motion of features in the counterjet as well as the main jet. This will provide a direct test of symmetric jet models, and further constrain relativistic beaming explanations of parsec-scale radio source asymmetries.

REFERENCES

Beall, J. H., et al. 1978, ApJ, 219, 836
Bridle, A. H., & Perley, R. A. 1984, ARA&A, 22, 319
Clarke, D. A., Burns, J. O., & Norman, M. L. 1992, ApJ, 395, 444
Fanaroff, B. L., & Riley, J. M. 1974, MNRAS, 167, 31P
Hui, X., Ford, H. C., Ciardullo, R., & Jacoby, G. H. 1993, ApJ, 414, 463
Jauncey, D. L., et al. 1995, Proc. Nat. Acad. Sci. USA, 92, 11368
Junkes, N., Haynes, R. F., Harnett, J. I., & Jauncey, D. L. 1993, A&A, 269, 29
Linfield, R. P. 1986, AJ, 92, 213

Preston, R. A., et al. 1996, in Extragalactic Radio Sources, in press
Ryle, M., & Longair, M. S. 1967, MNRAS, 136, 123
Scheuer, P. A. G., & Readhead, A. C. S. 1979, Nature, 277, 182
Tingay, S. J. 1996, Ph.D. thesis, Australian National Univ.
Tingay, S. J., et al. 1994, Aust. J. Phys., 47, 619
Vermeulen, R. C., Readhead, A. C. S., & Backer, D. C. 1994, ApJ, 430, L41
Walker, R. C., Romney, J. D., & Benson, J. M. 1994, ApJ, 430, L45